Journal of University of Science and Technology Beijing
Volume 9, Number 5, October 2002, Page 378

Materials

Numerical simulation of a sheet metal extrusion process by using thermal-mechanical coupling EAS FEM

Zhanghua Chen[1], *T.C. Lee*[2], *and C.Y. Tang*[2]

1) Applied Science School, University of Science and Technology Beijing, Beijing 100083, China
2) Department of Industrial System Engineering, The Hong Kong Polytechnic University, China
(Received 2002-02-13)

Abstract: The thermal-mechanical coupling finite element method (FEM) was used to simulate a non-isothermal sheet metal extrusion process. On the basis of the finite plasticity consistent with multiplicative decomposition of the deformation gradient, the enhanced assumed strain (EAS) FEM was applied to carry out the numerical simulation. In order to make the computation reliable and avoid hourglass mode in the EAS element under large compressive strains, an alterative form of the original enhanced deformation gradient was employed. In addition, reduced factors were used in the computation of the element local internal parameters and the enhanced part of elemental stiffness. Numerical results show that the hourglass can be avoided in compression region. In the thermal phase, the boundary energy dissipation due to heat convection was taken into account. As an example, a circular steel plate protruded by cylindrical punch was simulated. The step-wise decoupled strategy is adopted to handle coupling between mechanical deformation and the temperature variation. By comparing with the experimental results, the numerical simulation was verified.

Key words: enhanced assumed strain element; thermal-mechanical coupling process; hourglass mode

[*This work was financially supported by a research grant from the Hong Kong Polytechnic University (No.G-V694).*]

Recent experiments have shown that metals are susceptible to failure in the forms of shear banding and cracking during high speed impacting, machining and forming processes [1,2]. Especially, in sheet metal forming processes, the forming limit is governed by plastic instability and fracture following strain localization. In order to improve metal workability, considerable efforts have been devoted to explore the failure mechanisms in which the temperature gradient plays an important role to induce strain localization. In fact, heat generated from dissipated plastic work in metal forming processes. However, less time is available for the heat dissipating into surrounding medium by mans of heat transfer. This leads to the build-up of temperature gradients within regions undergoing large inhomogeneous deformations. Furthermore, the thermal softening effect will reduce the flow resistance and motivate flow localization. Decause the plastic deformation and temperature variation in sheet metal forming are interdependent, the temperature field and the distribution of mechanical quantities such as stress, strain as well as displacement must be solved simultaneously. Therefore, it is necessary to evaluate the influence of temperature by using the thermal-mechanical coupling technique.

In this paper, a numerical simulation of sheet metal extrusion process was conducted by using thermal-mechanical coupling finite element method. An enhanced strain finite element method was developed to solve the mechanical problem accompanying with successive remeshing operations. The standard Newton-Raphson iteration method as well as the corresponding consistent tangent operator was adopted to solve nonlinear elasto-plastic equations. In the thermal phase, the transient heat transfer finite element method together with the backward-Euler scheme was employed to determine the temperature field. Numerical solutions were verified by the recent experimental results.

1 Finite element formulation

In the present computation, the solution strategy for coupled problems is based on the staggered scheme proposed by Simo and Miehe [3]. This strategy yields an algorithmic decoupling of the symmetric thermomechanical equations within a typical time interval $[t_n, t_{n+1}]$ and these decoupled problems should be solved in the following steps: Firstly, the purely mechanical equation is solved by using large deformation elasto-plastic finite element method together with a global Newton-Raphson iterative algorithm at a fixed temperature Θ_n along with the given mechanical boundary

Corresponding author:Zhanghua Chen **E-mail**:czhhylchj@sina.com

conditions and the mechanical quantities is updated from reference configuration into current configuration after the iterative computation in this step. Secondly, the thermal equation is solved by means of a standard finite element method together with a global Newton-Raphson iterative algorithm at fixed configuration x_{n+1} along with the given thermal boundary conditions.

1.1 Enhanced strain element formulation

In order to overcome the lock deficiency that frequently exhibits in classic low order element, intensive research has been carried out to develop various improved elements. In the context of large deformation plasticity, the so-called enhanced strain formulation founded by Simo and Armero [4,5] has shown locking-free response in the near incompressible limit and this method can easily accommodate general inelastic constitutive relationship. However, it was subsequently observed that this element show hourglass modes for large strain, especially in the case of large compressive strain [6]. To avoid this drawback, a series of improved approaches have been proposed [7-11]. In the present study, following the recent work by Glaser and Armero [11], an enhanced assumed strain FEM programme has been developed to simulate metal forming processes. The key idea of this method is that the deformation gradient field is enhanced by a specially designed interpolation, which is an alterative basis of the original enhance d deformation gradient proposed by Simo and Armero [5]. Furthermore, for near incompressible problems such as metal forming, as proposed by Nagtegaal *et al.* [8], a kinematic restriction should be placed on the enhancement. This restriction condition can be interpreted as a requirement that the variation in the enhancement is orthogonal to a piece-wise constant pressure field. An approximate method to satisfy this condition is multiplicative decomposition of total deformation gradient, *i.e.*

$$\boldsymbol{F}_{n+1}=\frac{\partial \boldsymbol{x}_{n+1}}{\partial \boldsymbol{x}_n}=\Delta \boldsymbol{F}_{n+1}\cdot \boldsymbol{F}_n \tag{1}$$

Where subscript 'n' denotes the nth increment step, and $\Delta \boldsymbol{F}_{n+1}$ represents the current incremental deformation gradient:

$$\Delta \boldsymbol{F}_{n+1}=\frac{\partial \boldsymbol{x}_{n+1}}{\partial \boldsymbol{x}_n}+\hat{\boldsymbol{F}}_{n+1} \tag{2}$$

The field is $\hat{\boldsymbol{F}}_{n+1}$ constructed between the parametric domain and the deformed element domain:

$$\hat{\boldsymbol{F}}_{n+1}=\frac{J_0}{j}\boldsymbol{J}_0^{-T}\cdot H\cdot \boldsymbol{J}_0^{-1} \tag{3}$$

Where $\boldsymbol{J}_0$ denotes the Jacobian of the isoparametric mapping at the centroid of an element and j_0 is the determinant of $\boldsymbol{J}_0$, *i.e.*:

$$\boldsymbol{J}_0=\boldsymbol{J}(\xi)|_{\xi=0}=\frac{\partial \boldsymbol{x}_n}{\partial \xi}|_{\xi=0},\ j_0=\det(\boldsymbol{J}_0) \tag{4}$$

The enhanced interpolations are of the form:

$$H(\xi)=\begin{bmatrix}\xi\cdot\alpha_1 & \xi\cdot\alpha_2\\ \eta\cdot\alpha_3 & \eta\cdot\alpha_4\end{bmatrix} \tag{5}$$

Where α_k ($k=1, 2$) are the element local internal parameters. On the other hand, in the original formulations proposed by Simo *et al.*, the element local internal parameters are active to enrich the total deformation gradient field during the entire deformation process. However, due to the physical meaning of the internal parameters is not clear, it makes the remeshing work that is necessary for metal forming simulation more difficult because no suitable transformation method is available. In the present formulation, the enhanced interpolation field is constructed at the beginning of each increment so that mapping of the internal parameters can be avoided when remeshing is involved. With the incremental enhanced deformation gradient concept, the formulation of enhanced strain finite element can be developed from the two-field functional similar to the original formulation [11]. The linearized equations for Newton-Raphson iteration scheme can be expressed as:

$$\begin{bmatrix}\boldsymbol{K}_{dd} & \boldsymbol{K}_{\alpha d}^{T}\\ \boldsymbol{K}_{\alpha d} & \boldsymbol{K}_{\alpha\alpha}\end{bmatrix}\begin{Bmatrix}\Delta \boldsymbol{d}\\ \Delta\alpha\end{Bmatrix}=\begin{Bmatrix}\Delta \boldsymbol{f}^{c}\\ \Delta \boldsymbol{f}^{\alpha}\end{Bmatrix} \tag{6}$$

Where

$$\boldsymbol{K}_{dd}=\int_{V^e}\boldsymbol{B}^{T}\boldsymbol{c}\boldsymbol{B}\mathrm{d}V+\int_{V^e}\boldsymbol{G}^{T}\tau\boldsymbol{G}\mathrm{d}V \tag{7}$$

$$\boldsymbol{K}_{\alpha\alpha}=\int_{V^e}\boldsymbol{B}_{h}^{T}\boldsymbol{c}\boldsymbol{B}_{h}\mathrm{d}V+\int_{V^e}\boldsymbol{G}_{h}^{T}\tau\boldsymbol{G}_{h}\mathrm{d}V \tag{8}$$

$$\boldsymbol{K}_{\alpha d}=\int_{V^e}\boldsymbol{B}_{h}^{T}\boldsymbol{c}\boldsymbol{B}\mathrm{d}V+\int_{V^e}\boldsymbol{G}_{h}^{T}\tau\boldsymbol{G}\mathrm{d}V \tag{9}$$

$$\Delta \boldsymbol{f}^{c}=\boldsymbol{f}^{ext}-\int_{V^e}\boldsymbol{B}^{T}\tau\mathrm{d}V \tag{10}$$

$$\Delta \boldsymbol{f}^{\alpha}=\int_{V^e}\boldsymbol{B}_{h}^{T}\tau\mathrm{d}V \tag{11}$$

In the above equations, $\boldsymbol{B}$ and $\boldsymbol{G}$ are the linearized strain matrix and the nonlinear strain matrix, respectively. τ is the Kirchhoff stress tensor. The subscript 'h' represents the enhanced part of the matrix, $\boldsymbol{c}$ denotes the spatial elasticity tensor. On the other hand, in order to overcome the difficulty encountered under large compressive strains, reduced factors have been used in the computation of the element local internal parameters and the enhanced part of elemental stiffness. Therefore, the influence of the element local internal parameters can be weakened and energy distribution in element can also be adjusted. The modifications can be expressed as:

$$\Delta\alpha=-A^{*}\cdot\boldsymbol{K}_{\alpha\alpha}^{-1}\cdot(\Delta \boldsymbol{f}^{\alpha}+\boldsymbol{K}_{\alpha d}\cdot\Delta \boldsymbol{u}) \tag{12}$$

$$\boldsymbol{K}=\boldsymbol{K}_{dd}-B^{*}\cdot\boldsymbol{K}_{\alpha d}^{T}\cdot\boldsymbol{K}_{\alpha\alpha}^{-1}\cdot\boldsymbol{K}_{\alpha d} \tag{13}$$

Where $A^*=0.5$ and $B^*=0.3$ are the reduced factors. Their values are determined from numerical tests.

After the static condensation of element local parameters at elemental level, the assembled global stiffness equations can be directly solved. Both the return mapping algorithm for the multiplicative model of J_2-flow theory with isotropic hardening and the corresponding consistent tangent operator are the same as the one proposed by Simo and Armero [5]. During the iteration operations, the update of unknowns is accomplished following the increments of the nodal displacements:

$$\Delta \boldsymbol{u}^{(k+1)}=\Delta \boldsymbol{u}^{(k)}+\Delta \boldsymbol{d}^{(k+1)} \tag{14}$$

and the increments of the local internal parameters are expressed as:

$$\alpha^{(k+1)}=\alpha^{(k)}+\Delta\alpha^{(k+1)} \tag{15}$$

1.2 Heat generation and transfer

In sheet metal forming operation, the workpiece is subjected to plastic deformation and interfacial friction between the material and tools, which generate heat and result in material softening. In the present work, both strain-hardening and thermal-softening effects were taken into consideration. The thermoelastic (Gough-Joule) effect is ignored. The basic governing equation of heat transfer is expressed as:

$$\rho\cdot c\frac{\partial\theta}{\partial t}=k\cdot\left(\frac{\partial^2\theta}{\partial x^2}+\frac{\partial^2\theta}{\partial y^2}+\frac{\partial^2\theta}{\partial z^2}\right)+Q \tag{16}$$

Where c and ρ are the specific heat capacity and the density of the material, respectively. k denotes the heat conductivity and Q denotes the rate of heat generation. For cold metal forming process, the heat generated by plastic deformation work and boundary friction are expressed respectively as:

in the plastic region

$$Q=Q_m=\chi_p\sigma\varepsilon \tag{17}$$

and

at the contact boundary

$$Q=Q_f=\frac{1}{2}\chi_f\tau v \tag{18}$$

Where $\chi\approx0.85$ to 0.95 is a factor which describes the proportion of the dissipated energy converted into heat. Applying the principle of virtual work, the temperature distribution $\theta=\theta(x,y,z,t)$ in the work material as a function of time t can be obtained by solving the thermal energy equilibrium equation of heat transfer at the frozen (current) configuration:

$$[\boldsymbol{K}]\{\theta\}+[\boldsymbol{C}]\{\dot{\theta}\}=\{\boldsymbol{F}_m\}+\{\boldsymbol{F}_h\}+\{\boldsymbol{F}_f\} \tag{19}$$

$$\{\boldsymbol{F}_m\}=\int_\Omega[N]^T\cdot Q_m\cdot d\Omega \tag{20}$$

$$\{\boldsymbol{F}_h\}=\int_S h\cdot[N_S]^T[N_S](\{\theta_{ext}\}-\{\theta_S\})dS \tag{21}$$

$$\{\boldsymbol{F}_f\}=\int_S[N]^T\cdot Q_f dS \tag{22}$$

Where $[\boldsymbol{K}]$ and $[\boldsymbol{C}]$ are the heat conduction matrix and the heat capacity matrix, respectively. $\{\boldsymbol{F}_f\}$ is the interfacial friction heat flux vector, and $\{\boldsymbol{F}_h\}$ is the convective heat vector in which h denotes the convection coefficient. $\{\boldsymbol{F}_m\}$ is the mechanical dissipation heat flux vector. The effect of the boundary radiation is neglected in the present investigation.

2 FE model and boundary conditions

The target material of the workpiece is SS400 steel. The material constitutive equation has been determined through monotonic thermal tensile testing and the true stress versus the true strain relation has been corrected by using the well-known Bridgeman's correction approach for large strain. The relationship can be approximated by:

$$\sigma=[A\cdot(\bar{\varepsilon}^p+\bar{\varepsilon}_0)^n+H\bar{\varepsilon}^p]\cdot[1-\beta(\theta-\theta_0)]\quad\theta\le600℃ \tag{23}$$

Where $\bar{\varepsilon}^p$ denotes the equivalent plastic strain. The material properties and parameters used in equation (23) are listed as follows: Young modulus $E=210$ GPa; Poisson ratio $\nu=0.29$; stress coefficient $A=630$ MPa; initial equivalent strain $\bar{\varepsilon}_0=0.002$; strain hardening exponent $n=0.13$; linear strain hardening modulus $H=-23$ MPa; specific heat $c=460$ J/(kg·K^{-1}); density $\rho=7\,800$ kg/m^3; expansion coefficient $\alpha=1.5e^{-5}$ K^{-1}; heat conductivity $k=45$ W/(m·K^{-1}); dissipation factor $\chi=0.9$; thermal softening modulus $\beta=0.001\,4$ K^{-1}. The stress-strain curves at different temperatures with constant strain rate of 0.1 s^{-1} are illustrated in **figure 1**.

The sheet metal extrusion process, in which a 5 mm thick circular plate being protruded into a fixed die, is illustrated in **figure 2**. Both the punch and the die are considered as the rigid body. The edge-geometry of the tools is approximately simplified as a circular arc and its radius is assumed to be 0.1 mm. The coefficient of

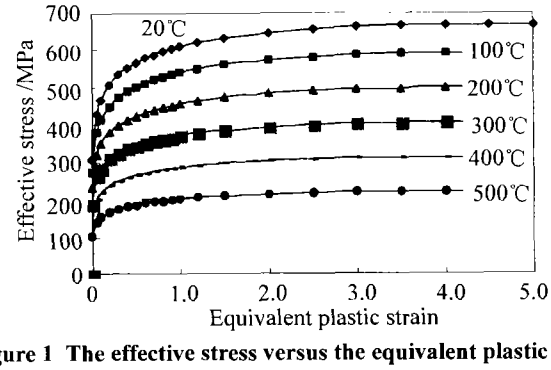

Figure 1 The effective stress versus the equivalent plastic strain curves at different temperatures.

friction at the interface between workpiece and tools is set to be 0.1. Due to the symmetry of the problem, only the right half of the workpiece is modeled. Since this sheet extrusion process is fulfilled in a short time (about 0.15 s), only the convective heat exchange between the workpiece and the forming lubricant has been taken into account in the thermal boundary condition. It is assumed that the normal heat flux defined by $q_n = h(\theta_w - \theta_s)$ on the entire contact boundary of the specimen. The constant convection coefficient is chosen as $h = 7.6\times10^{-3}$ N/(mm·s·K). The finite element model as well as the corresponding thermo-mechanical boundary condition is shown in **figure 3**. It is assumed that the contact surface is in good lubricating condition and a simple Coulomb model with a constant frictional coefficient of $f = 0.1$ is applied for calculating the friction at the interface between the tools and workpiece. Since the maximum friction cannot be greater than the shear yield stress, the friction is determined as follows:

$$\tau_f = f \cdot p \text{ if } \tau_f \le \tau_y \tag{24}$$

$$\tau_f = \tau_y \text{ if } \tau_f > \tau_y \tag{25}$$

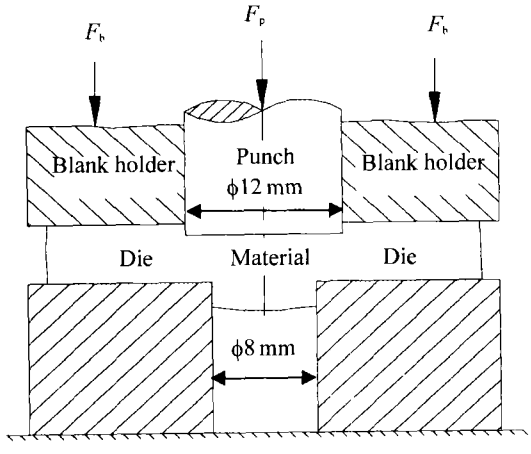

Figure 2 Schematic diagram of the sheet metal extrusion.

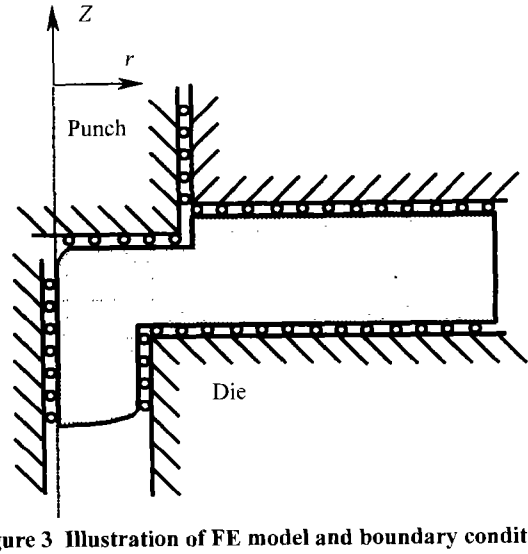

Figure 3 Illustration of FE model and boundary condition.

Where τ_f and τ_y denote the shear friction stress and the shear yield stress of material, respectively. The discrete mesh consists of about 2 160 axisymmetric four-node enhanced strain elements. To maintain the convergence in the iteration process of the Newton-Raphson scheme together with a line search solution procedure has been employed. It is emphasized that the line search is essential to ensure the computing convergence for a robust performance of Newton's method. In this simulation, the equal 100 displacement increments have been applied to simulate the punch penetrated 20% of the material thickness into the workpiece with a uniform punch velocity 15 mm/s.

3 Results and discussion

Initially, the specimen is at a homogeneous reference temperature $\theta_0 = 20$℃, which equals to the surrounding temperature θ_∞. At the early stage of deformation, the evolution of plastic strain is mainly concentrated near to the corner of the head of both the punch and the die. The progressive plastic deformation causes the local mesh within the region to be gradually degenerated and distorted and therefore, remeshing becomes inevitable. A total of 7 times remeshing operations have been carried out during the computation. A deformed mesh during the simulation is shown in **figure 4** and the enlargement of local mesh shows the remeshing effects. As the deformation proceeds, localized plastic deformation develops in the direction from the punch edge towards to the die edge. Due to localized plastic deformation and heat energy dissipates at the convection boundary, inhomogeneous distribution of the temperature field is therefore formed. The temperature gradient increases obviously at two regions, *i.e.* region A and region B as shown in **figure 5**. **Figure 6** shows the distribution of equivalent plastic strain of the workpiece at the finial deformation stage when the punch has extruded 20% into the thickness of material. The maximum plastic deformation zone is located at the shoulder edge (point C as shown in figure 6) at where the maximum equivalent plastic strain achieved 3.16. This tests were

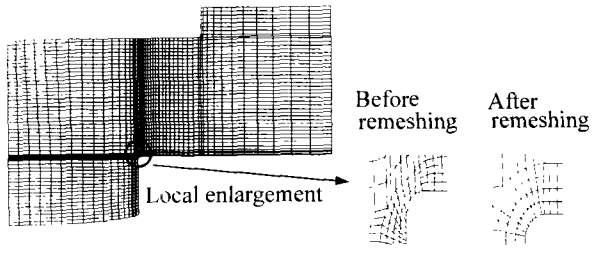

Figure 4 An illustration of the deformed mesh during the FE simulation of sheet metal extrusion process and enlargement of local mesh showing remeshing effects.

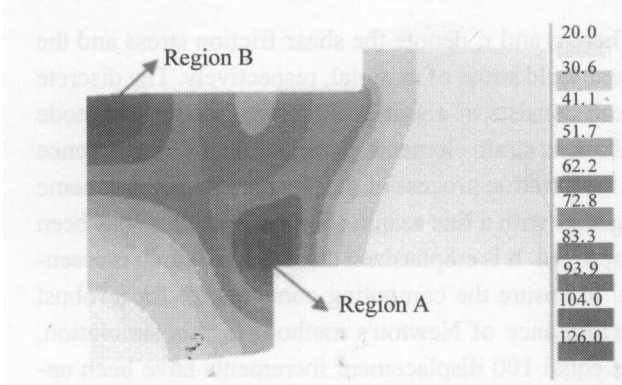

Figure 5 The temperature distribution (unit: ℃).

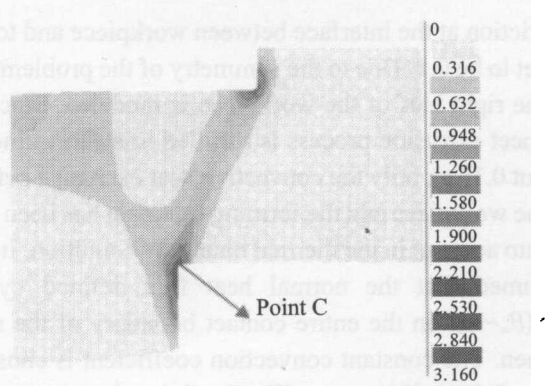

Figure 6 The equivalent plastic strain distribution.

performed at the ambient temperature (about 20℃) under good lubrication condition. **Figure 7** shows a picture of the extruded specimen with deformation grids. In this picture, the localized plastic deformation exhibites the 'M' pattern. By comparing the numerical result with the experimental observation, it is found that the deformation pattern is similar. It also reveals that the temperature gradient plays an important role to induce the strain localization.

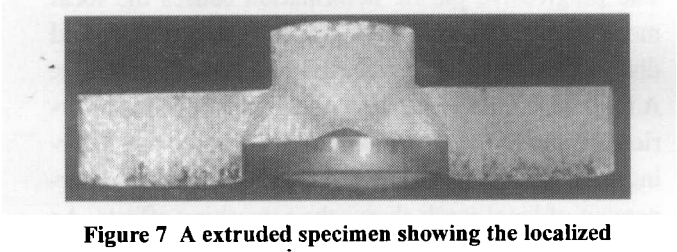

Figure 7 A extruded specimen showing the localized deformation.

4 Conclusions

To cope with the near-incompressible problems in metal forming processes, an improved enhanced strain finite element method has been used. Based on the large deformation plasticity of the multiplicative decomposition of the deformation gradient, this method exhibits a locking-free performance to simulate large deformation and a good performance to capture strain localization. It may be a kind of useful approach to simulation thermal-mechanical coupling metal forming processes.

When remeshing operation become inevitable, it may be appropriate to construct the enhanced deformation gradient in the rate form because the transferring of the local internal parameters can be avoided. However, this study shows that too many remeshing operations still led to accumulative error of the deformation gradient and it will make the computation unreliable.

References

[1] J.F. Kalthoff, Shadow optical analysis of dynamic shear fracture [J], SPIE, *Photomechanics and Speckle Metrology*, 814 (1987), p.531.

[2] E. Bayraktar and S. Altintas, Some problems in steel sheet forming processes [J], *J. Mater. Proc. Tech.*, 80-81 (1998), p. 83.

[3] M. Zhou, A.J. Rosakis, and G. Ravichandran, Dynamically propagation shear bands in prenotched plates-I. experimental investigations of temperature signatures and propagation speed [J], *J. Mech. Phys. Solids*, 44 (1996), p.981.

[4] J.C. Simo and C. Miehe, Associative coupled thermoplasticity at finite strain: formulation, numerical analysis and implementation [J], *Comput. Mech. Appl. Engng*, 98 (1992), p. 41.

[5] J.C. Simo and F. Armero, Geometrically non-linear enhanced strain mixed methods and the method of incompatible modes [J], *Int. J. Numer. Meth. Engng*, 33 (1992), p.1413.

[6] J.C. Simo, F. Armero, and R.L. Taylor, Improved versions of assumed enhanced strain tri-linear elements for 3D finite deformation problems [J], *Comput. Meth. Appl. Mech. Engng*, 110 (1993), p.359.

[7] E.A. Souza Neto, D. Peric, G.C. Huang, and D.R.J. Owen, Remarks on the stability of enhanced strain elements in finite elasticity and elastoplasticity [J], *Commun. Numer. Meth. Engng*, 11(1995), p.951.

[8] J.C. Nagtegaal, and D.D. Fox, Using assumed enhanced strain elements for large compressive deformation [J], *Int. J. Solids Struc.*, 33 (1996), p.3151.

[9] P. Wriggers and S. Reese, A note on enhanced strain methods for large deformations [J], *Comp. Meth. Appl. Mech*, 135 (1996), p.201.

[10] J. Korelc and P. Wriggers, Consistent gradient formulation for a stable enhanced strain method for large deformations [J], *Engng. Comput.*, 13(1996), p.103.

[11] S. Glaser and F. Armero, On the formulation of enhanced strain finite elements in finite deformation [J], *Engng. Comput.*, 14(1997), p.759.

[12] E.P. Kasper and R.L. Taylor, A mixed-enhanced strain method part II: geometrically nonlinear problems [J], *Computers & Structures*, 75(2000), p.251.